Biosensors and Bioelectronics 77 (2016) 409–415

Contents lists available at ScienceDirect

Biosensors and Bioelectronics

journal homepage: www.elsevier.com/locate/bios

A novel diagnostic biosensor for distinguishing immunoglobulin mutated and unmutated types of chronic lymphocytic leukemia

Ali A. Ensafi [a,*], Maryam Amini [a], Behzad Rezaei [a], Majid Talebi [b]

[a] Department of Analytical Chemistry, Faculty of Chemistry, Isfahan University of Technology, Isfahan 84156–83111, Iran
[b] Department of Biotechnology, College of Agriculture, Isfahan University of Technology, Isfahan 84156–83111, Iran

ARTICLE INFO

Article history:
Received 1 July 2015
Received in revised form
20 September 2015
Accepted 27 September 2015
Available online 30 September 2015

Keywords:
Chronic lymphocytic leukemia
IgVH mutation
ZAP70
DNA biosensor
Electrochemical impedance spectroscopy

ABSTRACT

In chronic lymphocytic leukemia (CLL), the immunoglobulin heavy-chain variable (IgVH) region may be mutated (Ig-mutated CLL) or unmutated (Ig-unmutated CLL); and the presence or absence of mutations in this region of CLL cells distinguishes two clinically distinct forms. It is important for physicians to distinguish between patients with Ig-unmutated CLL, where typically have more indolent disease with median survivals close to 25 years, and Ig-mutated CLL, where have more aggressive disease with median survivals around eight years. In this work, a biosensor capable of diagnosis and distinguishing between these two types of CLL was reported. The biosensor was fabricated by modifying a gold electrode with gold nanoparticles (AuNPS) followed by coating of ZAP70 oligonucleotide probe on the surface to detect specific sequence of ZAP70 gene. ZAP70 could predict the IgVH mutation status and is a good marker for differentiating Ig-mutated and Ig-unmutated CLL and serve as prognostic marker. First, we focused on achieving hybridization between probe and its complementary sequence. Hybridization between probe and target was determined with electrochemical impedance spectroscopy (EIS). Then, our efforts turned to optimize the conditions for the detection of any point mutation and also to maximize the selectivity. Under optimal conditions, the biosensor has a good calibration range between 2.0×10^{-14} and 1.0×10^{-9} mol L^{-1}, with ZAP70 DNA sequence detection limit of 4.0×10^{-15} mol L^{-1}. We successfully detect hybridization first in synthetic samples, and ultimately in blood samples from patients. Experimental results illustrated that the nanostructured biosensor clearly discriminates between mutated and non-mutated CLL and predict the IgVH mutation status, which it has been considered as the single most informative stage independent prognostic factor in CLL.

1. Introduction

Cancer research is one of the most important research areas in the medical sciences. Cells become cancer cells largely because of changes in their genes that called mutations. Mutations play an important role in the development of cancer. The main conventional methods for detecting mutation are polymerase chain reaction (PCR) followed by restriction enzyme analysis (Zhang et al., 2015), ligase chain reaction (Bia et al., 2015) and nick translation PCR with fluorogenic DNA probes (Lee et al., 1993). These detection schemes are mostly based on the coupling of gel electrophoresis and radioisotopic labeling and are thus not suitable for automation (Ozsoz et al., 2003). The possibility of using minimally invasive analytical instruments to monitor genomic mutation provide great advances in cancer research. Biosensors have emerged as a new technique for monitoring mutation. The real success in the development of a reliable sensor depends on the ability to design powerful instrumentation that will facilitate efficient signal transduction from the biological process that occurs in the cellular environment (Sadik et al., 2009).

Modern electrochemical DNA sensors, have recently demonstrated great potential for monitoring cancer-related DNA mutations (Zhu et al., 2015; Akhavan et al., 2012). Electrochemical methods, when compared to the conventional methods for DNA analysis (e.g., fluorescence microscopy, radioactivity measurements, quartz crystal microbalance and surface plasmon resonance) are straightforward and sensitive and do not require sophisticated instrumentation. Consequently, they are appropriate for the development of inexpensive and portable devices for disease diagnoses (Alfonta. et al., 2000). To construct the DNA based biosensor for detection of specific DNA sequence; the single-strand functional nucleic acid that called probe is immobilized on the solid support and coupled with specific single strand DNA (the target) within the analyte. The complementary strands anneal to one another in Watson–Crick base pairing. The specific and selective detection of DNA sequences, with single-base mismatch

* Corresponding author. Fax: +98 31 33912350.
E-mail addresses: ensafi@cc.iut.ac.ir, aaensafi@gmail.com (A.A. Ensafi).

http://dx.doi.org/10.1016/j.bios.2015.09.063
0956-5663/

detection ability, is a major challenge to address in DNA biosensing (Keller and Manak, 1993).

One of the human diseases caused by mutations is chronic lymphocytic leukemia (CLL). CLL is a biologically heterogeneous disease of the lymphoid system that is characterized by the progressive and irreversible growth of mature deficient B-cells and various genomic aberrations and mutations (Scupoli and Pizzolo, 2015). It is a disease of aged populations and the most common adult leukemia in the Western world, with an estimated incidence of 5.8 cases per 100,000 men per year and 3.0 per 100,000 women per year (Campregher and Hamerschlak, 2014; Strefford, 2015). It is estimated that there will be ~14,620 new cases of CLL and ~4650 deaths due to the disease in the United States alone in 2015 (Esencay and Hamad, 2015). It has been recently proven that 50–60% of patients with CLL have somatic mutations in the immunoglobulin heavy chain variable region (IgVH) gene (Šoljić et al., 2013). Patients with CLL, who express mutated IgVH genes as defined above, typically have more indolent disease and a better prognosis with median survivals close to 25 years, while those with unmutated IgVH genes often have more aggressive disease and a poorer prognosis with median survivals around 8 years (Moreno and Montserrat, 2008; Montserrat, 2006). Unlike other prognostic factors, IgVH gene mutation status does not change during the disease, but, due to the complexity of the analysis method, it is unsuitable for routine clinical practice (Rassenti et al., 2004).

Although the IgVH gene mutation status is a powerful prognostic indicator, much attention has focused on finding surrogate markers for the mutation status that could be more rapidly detected than the time-consuming sequencing that is necessary to determine the mutation status (Tobin and Rosenquist, 2005). Rosenwald et al. (2001) found more than 100 genes differentially expressed between the Ig-mutated and Ig-unmutated CLL subtypes with high statistical significance. The most differentially expressed gene was ZAP-70, which encodes a tyrosine kinase. The association of the IgVH gene mutation status, revealing that ZAP-70 can predict the IgVH gene mutation status with a high accuracy in CLL (Crespo et al., 2003). These studies suggest that ZAP-70 could function as a surrogate marker for IgVH gene mutation status in CLL, which would enable a faster analysis to predict prognosis than the IgVH gene analysis.

There are several methods to quantify ZAP-70 including: polymerase chain reaction (PCR), immunoblotting, immunohistochemistry, fluorescence in-situ hybridization (FISH) analysis and flow cytometry (Slack et al., 2007, Wang et al., 2012, Put et al., 2009, Vroblova et al., 2012, Matthews et al., 2004, Moreno and Montserrat, 2010). Use of flow cytometry for ZAP-70 detection seems to be advantageous as this technique enables us to assess the presence of ZAP-70 separately on CLL clone, T-cells and NK-cells. But the remarkable thing is that, in general, the above methods are costly and time consuming methods compared to simpler methods such as label free electrochemical method. Also, while the presence and absence of IgVH mutation state is currently the gold-standard prognostic factor, but this distinction is labor-intensive and costly (Wang et al., 2012). Generally, analysis of IgVH mutation state is a relatively expensive and time-consuming test with restricted availability. Thus providing a simple, reliable and low cost method that can distinguish between the Ig-mutated and Ig-unmutated CLL subtypes within the shortest possible time has particular importance.

In this paper, a label-free electrochemical DNA biosensor, based on ZAP70 probe, has been fabricated to detect specific sequence of ZAP70 gene, which is highly associated with CLL cancer and IgVH gene mutation status. The biosensor was fabricated by modifying a gold electrode with gold nanoparticles (AuNPs) followed by coating of ZAP70 oligonucleotide probe on the surface to detect specific sequence of ZAP70 gene. A probe ss-DNA (25–mer) modified with –SH is self-assembled onto the surface of the modified electrode. The target DNA, which contains complementary sequence to the probe DNA, would be captured by the probe DNA through hybridization. The ZAP70 oligonucleotide, which is complementary with another part of the target DNA would be hybridized. We also exploit the impedance spectroscopy as a platform for reagent-less DNA sensing assay. The biosensor was employed for the diagnosis and distinguishing of Ig-mutated and Ig-unmutated CLL conditions and the IgVH mutation status in patients. To the best of our knowledge, up to the present time, there is no electrochemical study dealing with sensing of ZAP70 gene level and the distinction between Ig-mutated and Ig-unmutated CLL conditions.

2. Experimental

2.1. Chemicals

All solutions were prepared using reagent grade chemicals and doubly distilled water was used through the work. Hydrogen tetrachloroaurate(III) ($HAuCl_4$, $4H_2O$) and potassium nitrate (KNO_3) were purchased from Merck (Darmstadt, Germany). All oligonucleotides were synthesized and purified in Takapu Zist Institute (Tehran, Iran). All oligonucleotides were diluted with ultrapure water and stored as a stock solution in a freezer. The following five oligonucleotides sequences were used in this study:

ZAP70 probe (p_{25})	5′-SH-CCCTGCGCCAGCACGCATAACGT-3′
ZAP70 target (C_{25})	5′-ACGTTATGCGTGCTGGCGCAGGG-3′
Target with longer sequence (C_{40})	5′-ACGTTATGCGTGCTGGCGCAGGGGTGTATCCATCT-GAGTT-3′
Mismatch sequence (M_{25})	5′-ACGTGATGCGTGCTGGCGCAGGG-3′
Mismatch with longer sequence (M_{40})	5′-ACGTGATGCGTGCTGGCGCAGGGGTGTATCCATCT-GAGTT-3′

All solutions were prepared with Milli-Q water (18 MΩ cm resistivity) from a Millipore system.

2.2. Apparatus

Electrochemical measurements were performed using Vertex (Potentiostat/galvanostat with optional FRA/EIS) from Ivium, connected to a standard one-compartment three-electrode cell. The reference electrode was Hg/Hg_2Cl_2 (3 mol L^{-1} KCl) and the counter electrode was a platinum wire. The modified gold electrode was used as a working electrode through the work. Metrohm pH–meter (Model 827) with a glass electrode (Corning) was used to adjust the pH of solutions.

2.3. Preparation of the modified gold electrode with AuNPs (AuNPs/

AU electrode)

Preparation of AuNPs/Au electrode was performed according to our previous work (Ensafi et al. 2011). In this regard, firstly the surface of the gold disk electrode (2.0 mm in diameter) was polished to a mirror-finished with slurry alumina on a polishing cloth for 2 min. The polished electrode was immersed in a piranha solution (7:3, sulfuric acid/hydrogen peroxide) for 1 min and then cleaned ultrasonically in a 1:1 mixture of ethanol and water, to remove any possible surface contaminate. The gold electrode was then subjected to potential cycling (−0.20 to +1.50 V, 50 mV s^{-1}) in 0.5 mol L^{-1} sulfuric acid solution until a stable cyclic voltamogram was obtained. The pretreated electrode was immersed into 3.0 mmol L^{-1} $HAuCl_4$ solution, containing 0.1 mol L^{-1} KNO_3 as an electrolyte for 180 s, and the electrochemical deposition was conducted at −200 mV by single potential mode (Li et al., 2005). Inert atmosphere were used in all steps, using nitrogen gas.

2.4. Preparation of aptasensor (P_{25}/AuNPs/AU electrode)

In order to construct the P_{25}/AuNPs/Au electrode, the AuNPs/Au electrode was placed in a moist chamber and 5.0 μL of the probe solution (P_{25}) was dropped on a cleaned surface of the AuNPs/Au electrode at room temperature. Then the surface of electrode was dried in moist chamber overnight and was washed with sterile water to remove the probe that was not connected to the electrode surface.

2.5. Hybridization and electrochemical measurements of the aptasensor

The hybridization procedure was performed by dropping 5.0 μL of the target solution (C_{25}) on the surface of aptasensor (P_{25}/AuNPs/Au electrode) at 46 °C. In order to adjust the temperature of hybridization, the P_{25}/AuNPs/Au electrode was placed in a closed moist chamber and then transferred to a water bath. Then, the water bath was set to the desired temperature and the target solution (C_{25}) was seeped on the surface of the heated P_{25}/AuNPs/Au electrode for 90 min. The modified electrode in this step was named as C_{25}–P_{25}/AuNPs/Au electrode. It should be noted that the target solution (C_{25}), before the dropping, is heated in water bath to the desired temperature or in other words the electrode surface and target solution (C_{25}) before seeping were completely isothermal.

2.6. Electrochemical impedance spectroscopy and cyclic voltammetry

Cyclic voltammetry (CV) and electrochemical impedance spectroscopy (EIS) measurements were carried out in 5.0 mmol L^{-1} $[Fe(CN)_6]^{3-/4-}$, as a redox probe, in 0.1 mol L^{-1} KCl. The impedance spectra were recorded within the frequency range of 0.005 to 10^5 Hz. The amplitude of the applied sine wave potential, in each case, was 10 mV. The cyclic voltammogram was recorded using a scan rate of 100 mV s^{-1}. The difference in the anodic to cathodic peak potential separation was evaluated.

2.7. DNA extraction from plasma

We collected blood samples from two CLL patients and one healthy volunteer in collection tubes containing lithium heparin. DNA extraction was done with a modified Miller method (Miller et al., 1998) as follows: 300 μL of a whole blood plus 900 μL erythrocyte (RBC) lysis solutions were completely shaken for 10 min. Then, the mixture was centrifuged at 2000 rpm for 5 min. The supernatant was discarded and the precipitate was kept and washed 2 times with 900 μL erythrocyte lysis solution (for 10 min) and centrifuged at 2000 rpm for 5 min. Then, 400 μL leukocyte (WBC) lysis buffer was added to the final precipitate of the last step and well shaken, then 41 μL SDS (10%) was added to it. 10 μL proteinase K (cat. No. 1073930010; Merck) was added to the mixture and was kept in 60 °C for 60 min. 100 μL NaCl (saturated, 5 mol L^{-1}) was added to the mixture and the resulted mixture was kept 10 min at −20 °C, and then 20 min at 4 °C and centrifuged at 13,000 rpm. 400 μL of the supernatant was separated and kept in a vial. 400 μL isopropanol was added to the resulted mixture and the precipitated DNA was kept at −20 °C for 15 min and then it was centrifuged at 13,000 rpm at 4 °C for 10 min and the supernatant was discarded. The resulted product was dried 1 h in the lab temperature. Finally, distilled water was added as required and the DNA was ready to keep in a fridge or freezer.

The quality and quantity of the extracted DNA were evaluated by standard 0.7% agarose gel electrophoresis and spectrophotometery, respectively. The DNA was digested by 5 restriction enzymes to produce different kinds of fragments as the enzymes work. The final concentration of the extracted DNA was 300 μmol L^{-1}.

2.8. Procedure

Detection of ZAP70 gene (target sequence C_{25}) was carried out by means of EIS. The P_{25}/AuNPs/Au electrode was prepared according to Section 2.3. Then, the impedimetric response (R_{ct}) of P_{25}/AuNPs/Au electrode was recorded and named as R_1. In second stage, the target sequence (C_{25}) was seeped on the surface of P_{25}/AuNPs/Au electrode at 46 °C and after drying the impedimetric response of C_{25}–P_{25}/AuNPs/Au electrode was recorded and named R_2. The analytical signal ($(R_2-R_1)/R_1$ ($\Delta R/R_1$)) represented the difference in the R_{Ct} of ds-DNA (R_2) and ss-DNA (R_1). Prior to measurement the ZAP70 gene (target sequence C_{25}), all effective parameters in construction and measurement were evaluated and optimized with EIS method. In final stage, in order to assess the selectivity of our work, the effect of longer targets and mismatch sequences was evaluated and finally the amount of ZAP70 gene in patients was measured. Overview of the work is shown in Scheme 1.

3. Result and discussion

3.1. Surface characterization and hybridization detection

Characterization of the surface was performed by means of SEM, CV and EIS methods. Deposition of AuNPs on the surface of Au electrode was performed according to our previous work (Ensafi et al., 2011). The results confirmed that 180 s (as deposition time) is a suitable time for AuNPs preparation with a uniform size, high density, and good shape. As deposition time is increased, serious aggregation of the gold nanoparticles happened. At shorter deposition time, the electrode surface has a smaller size particles, but with lower density. So, the time of 180 s was selected and used for AuNPs deposition. Fig. 1 shows the SEM image of Au-electrode before (A) and after (B) deposition of AuNPs. The obtained results using SEM indicate that gold nanoparticles are well established on the electrode surface.

Electrochemical impedance spectroscopy (EIS) is highly suitable for measuring electrode surface changes and has been considered as a label-free strategy for rapid bioanalysis (Ensafi et al., 2014, 2013). Using EIS, each step can be readily detected by monitoring the change in charge transfer resistance (R_{ct}). As shown in Fig. 2A (b), after stabilization of the AuNPs, the amount of charge transfer resistance (R_{ct}) decreases due to excellent

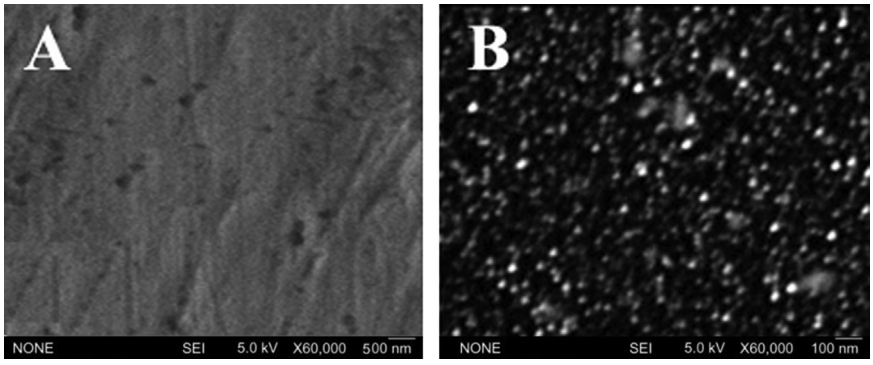

Fig. 1. SEM images of the (A) Au and (B) AuNPs/Au electrode.

conducting capability and high surface to volume ratio of AuNPs. The AuNPs due to good biological compatibility are used as suitable bed for immobilization of biological species (Ali et al., 2014). Our studies proved that after immobilization of probe (P_{25}), the amount of R_{ct} (diameter of semicircle) increases as shown in Fig. 2A (c). The increase in R_{ct} is due to the repulsion between negatively charged DNA and the negative redox indicator ion, the $[Fe(CN)_6]^{3-/4-}$. After hybridization of complementary DNA (C_{25}), the interfacial R_{ct} increased further to a much larger value (Fig. 2A (d)). This phenomenon is due to generation of an insulator layer on AuNPs/Au electrode and also increasing the negative charge on the electrode surface. Fig. 2A (e) is EIS response of P_{25}/AuNPs/Au electrode that interacted with 25-mer mismatch (M_{25}) sequence to form M_{25}–P_{25}/AuNPs/Au electrode. As see in this figure, the R_{ct} and the graph related to P_{25}/AuNPs/Au electrode is exactly equal to R_{ct} and the graph of M_{25}–P_{25}/AuNPs/Au electrode. These results confirm that there is no effective interaction between M_{25} sequence and P_{25} sequence on the surface of AuNPs/Au electrode.

It is not unexpected that P_{25} sequence does not cover the entire surface of AuNPs/Au electrode and certainly there are pores on the adsorbed layer without any linkage with p_{25} sequence which may lead to misleading results and non-specific adsorption of oligonucleotides or other molecules on the uncovered areas. To investigate this subject, C_{25}/AuNPs/Au electrode was fabricated by dropping the target sequence C_{25} on the surface of AuNPs/Au electrode under the condition in Section 2.4 and dried. The value of R_{ct} related to C_{25}/AuNPs/Au and AuNPs/Au electrode was equal completely. These observations demonstrate that sequences without thiol groups cannot be bonded to the surface of gold nanoparticles and therefore empty spaces on the electrode surface after immobilization of P_{25} sequence does not cause interference to hybridization.

Fig. 2B shows typical cyclic voltamograms of $[Fe(CN)_6]^{3-/4-}$ at the different electrodes surface. A pair of well-defined oxidation and reduction peaks are observed at the AuNPs/Au electrode with a peak-to-peak separation of 80 mV (Fig. 2B(a)). After immobilization of P_{25} sequence on the surface of AuNPs/Au electrode, the peak current decreased dramatically and the peak-to-peak separation increased quite conspicuously (Fig. 2B(c)). Our results showed that after hybridization, the peak current of $[Fe(CN)_6]^{3-/4-}$ decreased and the peak-to-peak separation reached to 180 mV. In addition, the voltamograms of M_{25}–P-$_{25}$/AuNPs/Au electrode and C_{25}/AuNPs/Au electrode were superimposed on voltamograms of P_{25}/AuNPs/Au electrode and AuNPs/Au electrode, respectively, that confirms obtained results from EIS technique (figures not shown).

In order to achieve the best results, several parameters such as concentration of probe (p_{25} sequence), temperature of hybridization and hybridization time were optimized. To investigate the effect of the probe concentration on the sensitivity, different solutions of P_{25} sequence in the concentration range of 25.0–150.0 μmol L^{-1} were selected for preparation of P_{25}/AuNPs/Au electrode. The prepared P_{25}/AuNPs/Au electrodes (with different concentration of P_{25} sequence) were dried overnight and then, their impedimetric responses (R_{ct}) were recorded. The results (Fig. 3A) showed that the R_{ct} of P_{25}/AuNPs/Au electrode increased

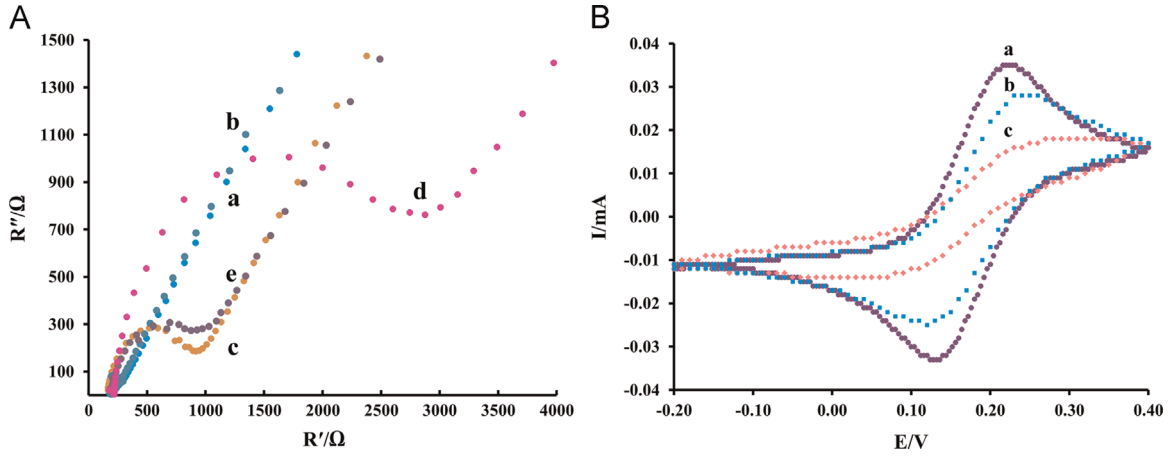

Fig. 2. (A) Nyquist diagrams of the bare gold electrode (a), the AuNPs/Au electrode (b), the P_{25}/AuNPs/Au electrode (c), the C_{25}–P_{25}/AuNPs/Au electrode (d) and the M_{25}–P_{25}/AuNPs/Au electrode (e) in a solution containing 5.0 mmol L^{-1} $[Fe(CN)_6]^{3-/4-}$ and 0.1 mol L^{-1} KCl. (B) Cyclic voltammogram curves of the AuNPs/Au electrode (a), the P_{25}/AuNPs/Au electrode (b), and the C_{25}–P_{25}/AuNPs/Au electrode (c) in a solution containing 5.0 mmol L^{-1} $[Fe(CN)_6]^{3-/4-}$ 0.1 mol L^{-1} KCl using a scan rate of 100 mV s^{-1}. CV measurements were carried out at scan rate of 100 mV s^{-1} between −0.20 and +0.40 V; EIS conditions: polarization potential: 0.15 V, frequency: 0.005–10^5 Hz, and amplitude: 10 mV.

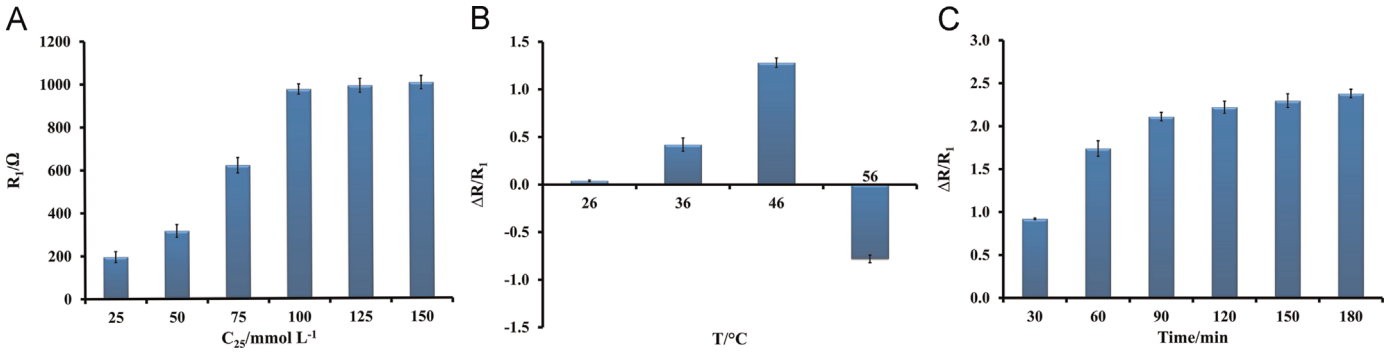

Fig. 3. Effect of the probe concentration (P_{25} sequence) (A), temperature of hybridization (B) and hybridization time (C) on the impedimetric electrochemical response. EIS conditions: polarization potential: 0.15 V, frequency: 0.005–10^5 Hz, and amplitude: 10 mV.

by increasing the P_{25} sequence concentration up to 100.0 μmol L^{-1}, and then leveled off. Therefore this concentration was selected to construct the P_{25}/AuNPs/Au electrode during the study. In the next stage of optimization, the effect of hybridization temperature on the $\Delta R/R_1$ was evaluated. For this purpose, the P_{25}/AuNPs/Au electrodes were prepared according to Section 2.3. The hybridization procedure was performed by dropping the 5.0 μL of 0.1 nmol L^{-1} target solution (C_{25}) on the surface of P_{25}/AuNPs/Au electrode at temperature range between 26–56 °C for 40 min in a hot water bath and then dried in room temperature, overnight. Then, the impedimetric responses of C_{25}–P_{25}/AuNPs/Au electrodes were recorded. Our results (Fig. 3B) showed that the amount of $\Delta R/R_1$ for temperature of 26 °C is very low. In other word, the value of R_{ct} of P_{25}/AuNPs/Au electrode, after hybridization at 26 °C, is approximately equal to the response related to P_{25}/AuNPs/Au electrode before hybridization. This means that, at this temperature, hybridization process was not done. Furthermore, our results showed that the amount of $\Delta R/R_1$ was maximized at 46 °C, therefore this temperature was selected as an optimum temperature for the hybridization.

In the final stage of the optimization, the hybridization time was evaluated and optimized. In order to optimize this parameter, 5.0 μL of 0.1 nmol L^{-1} target solution (C_{25}) was dropped on the surface of P_{25}/AuNPs/Au electrode and hybridization process was performed in a time range between 30–180 min. Then, the surfaces of C_{25}–P_{25}/AuNPs/Au electrode was dried in room temperature overnight and their impedimetric responses (R_{ct}) was recorded. Our results (Fig. 3C) showed that the amount of $\Delta R/R_1$ was maximized in 90 min as hybridization time and then leveled off. So this time was selected for hybridization process during the work.

The performance of P_{25}/AuNPs/Au electrode was assessed by varying C_{25} target concentration (Fig. 4). The results showed that the impedimetric signal ($\Delta R/R1$) increased linearity with the target concentration up to 1.0 nmol L^{-1} and then remained constant with further increase of the target concentration, which indicates that all the immobilized probes on the electrode surface have been involved in hybridization at the concentration of 1.0 nmol L^{-1}. The impedimetric signal ($\Delta R/R1$) was linearly depend on the concentration of the target oligonucleotide sequence of the ZAP70 between 2.0×10^{-14} and 1.0×10^{-9} mol L^{-1} (R^2=0.9949). The detection limit was 4.0×10^{-15} mol L^{-1} based on the ratio of signal-to-noise of 3. In addition, the ZAP70 gene was reproducibly measured in all concentrations with coefficients of variation less than 8%, which indicated an acceptable reproducibility.

One of the advantages with the use of aptasenors include easy regeneration of the biosensor by changing temperature or pH to break the aptamer–target interactions. Generally, highly alkaline environment would destabilize the immobilized aptamer or affect the interaction between aptamer and its target (Chun et al., 2013).

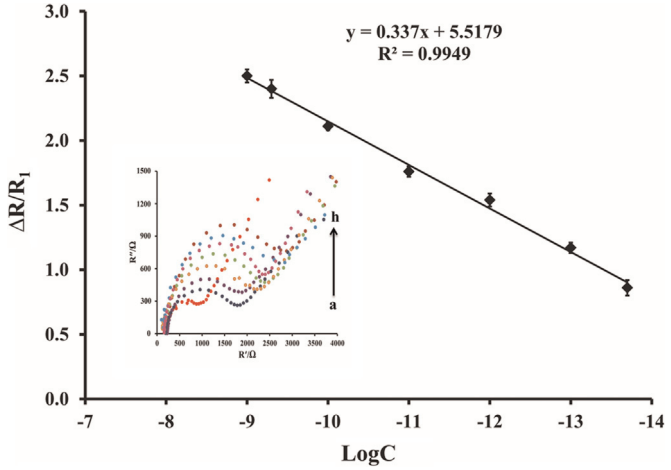

Fig. 4. Calibration plot of the DNA target: Inset shows the EIS signals. EIS conditions: polarization potential: 0.15 V, frequency: 0.005–10^5 Hz, and amplitude: 10 mV.

In order to investigate the regeneration of the sensor, the C_{25}–P_{25}/AuNPs/Au electrode was socked in 0.01 mol L^{-1} NaOH solution for 5 min and washed with sterile water (Zhang and Zhang, 2008). Then, 5.0 μL of C_{25} target solutions (2×10^{-13} and 2×10^{-10} mol L^{-1}) were dropped separately on the P_{25}/AuNPs/Au electrodes under the mentioned condition in Section 2–4 and the impedimetric responses ($\Delta R/R_1$) were recorded. Our results showed that the imepedimetric signal ($\Delta R/R$) obtained from the regenerated sensor is in good agreement with the results from freshly prepared P_{25}/AuNPs/Au electrodes. The generation process was repeated for second and third times too. The results of the fresh prepared sensor, first, second and third regenerated P_{25}/AuNPs/Au electrodes are shown in Fig. 5A. As can be seen in this figure, the impedimetric signals ($\Delta R/R1$) of the fresh prepared, first and second regenerated sensors have approximately equal amounts but there is a large different between the impedimetric responses ($\Delta R/R1$) of the third regenerated electrode and fresh prepared P_{25}/AuNPs/Au electrode. This difference could be due to DNA dislodge from the surface after soaking in soda solution in three times, so that the impedimetric response of the sensor after third generation is similar to AuNPs/Au electrode. Therefore P_{25}/AuNPs/Au electrodes can be regenerated twice and after three times recovery is not applicable.

In addition, the stability of the genosensor was also studied by testing impedimetric response over 30 days of storage at 4 °C. No obvious and significant change in impedimetric response of P_{25}/AuNPs/Au electrode was found over 20 days.

In order to test the selectivity of the fabricated aptasensor, 0.1 nmol L^{-1} of different sequences containing short mismatch

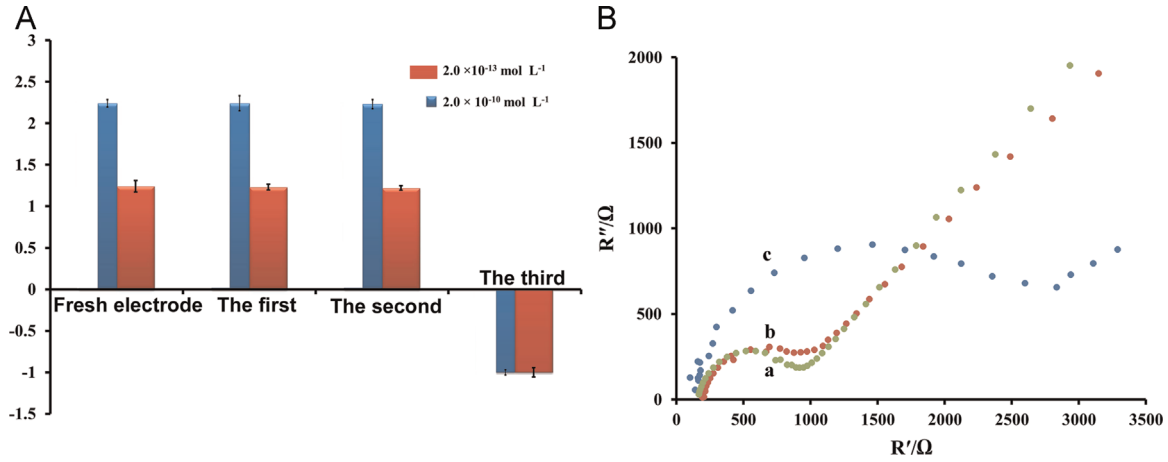

Fig. 5. (A) EIS response ($\Delta R/R_1$) of fresh P_{25}/AuNPs/Au electrode, the first, second and third regenerated P_{25}/AuNPs/Au electrodes after dropping two different target concentrations (2.0×10^{-10} and 2.0×10^{-13} mol L^{-1}). (B) Impedimetric electrochemical responses of P_{25}/AuNPs/Au electrode after dropping of 1.0×10^{-9} mol L^{-1} (a) M_{25}, (b) M_{40} and (c) C_{40} on the surface of the electrode. EIS conditions: polarization potential: 0.15 V, frequency: 0.005–10^5 Hz, and amplitude: 10 mV.

sequence (M_{25}) (Guanine was replaced with thymine on base no. 5), long mismatch sequence (M_{40}) and long complementary sequence (C_{40}) were dropped on the surface of P_{25}/AuNPs/Au electrodes separately and the impedimetric responses ($\Delta R/R_1$) were recorded. The Nyquist plots of P_{25}/AuNPs/Au electrode, after hybridization with (a) M_{25} and (b) M_{40} sequences (Fig. 5B) show that the R_{ct} related to C_{40}–P_{25}/AuNPs/Au electrode is higher than R_{ct} of P_{25}/AuNPs/Au electrode. Generally it can be said that, the aptasensor had no interaction with M_{25} and M_{40} sequence and these results suggest that the aptasensor has higher selectivity for the complementary sequences *vs.* the mismatch one.

3.2. Analytical application

In order to show the applicability of the biosensor, beside the synthetic oligonucleotides, target DNA could be analyzed by the constructed DNA biosensor in real samples. Another attractive feature of the developed method is that it can be used for assaying the ZAP70 gene level precisely from serum samples. The analysis results of the determination of ZAP70 gene in the spiked human serum sample showed that for human unfragment DNA, after adding 4.0×10^{-11} mol L^{-1} ZAP70, $4.2(\pm0.3)\times10^{-11}$ mol L^{-1} was found. In addition, for the analysis of ZAP70 gene in the spiked human serum sample, it was shown that for human fragment DNA, after adding 4.0×10^{-11} mol L^{-1} ZAP70, $3.8(\pm0.2)\times10^{-11}$ mol L^{-1} was found. The results indicated that the developed approach has high accuracy in the measuring ZAP70 gene level. These observations substantially demonstrate that the method could be potentially used for detection of ZAP70 gene in real clinical samples.

3.3. Distinguish of types of CLL in patient serum samples

The ultimate objective of the presented ZAP70 gene impedimetric biosensor is to employ it for the diagnosis and discrimination of Ig-mutated and Ig-unmutated CLL conditions in patients. Therefore, we examined ZAP70 gene concentrations in both types of CLL patient serum samples received from Al-Mahdi Laboratory (Isfahan, Iran). Total DNA extraction of the blood cells of CLL patient was performed, as detailed in the Experimental section. Table 1 compares the results of the analysis of ZAP70 gene in different CLL patient samples. The results showed that R_{ct} would not change after the dropping of DNA sample of patients 1 & 2 (patients with mutated immunoglobulin genes) on the surface of the biosensor, whereas it changed for patients 3 & 4 (patients with unmutated immunoglobulin genes). As a result, hybridization was not detected in the serum extracted from CLL patients with mutated immunoglobulin genes, showing that, there is not ZAP70 gene in the samples. This distinguishes types of CLL patients from ones, since the samples without the Ig mutation have detectable ZAP70, whereas those with the Ig mutation do not. Given the clinical differences between Ig-mutated and Ig-unmutated CLL, it would be beneficial to incorporate this distinction into clinical diagnosis of patients with CLL. The results show that electrochemical impedance spectroscopy beside the biosensor is one of the best candidates for diagnosis and distinguish of Ig-mutated and Ig-unmutated CLL conditions in patients.

Table 1
Detection of the ZAP70 related gene in extracted DNA from blood cells of CLL patients.

Sample	Spiked (pmol L^{-1})	Determined[a] (pmol L^{-1})	Recovery (%)	RSD[b] (%)
Ig-mutated CLL				
Patient 1	0.0	Undetected		
	5.0	4.8	96.6	5.2
Patient 2	0.0	Undetected		
	5.0	4.7	93.6	4.2
Ig-unmutated CLL				
Patient 3	0.0	1.4		
	5.0	6.1	95.3	6.5
Patient 4	0.0	0.65		
	0.50	1.23	106.9	5.5

[a] Mean of five measurements.
[b] Relative standard deviation.

4. Conclusions

Considering the rapid growth of both types of CLL worldwide and associated lethal complications, a simple and accurate detection is quite useful. Since the initial discovery as ZAP70 that associated with IgVH mutation status, the prognostic importance of ZAP70 in CLL has been clarified. The results presented above demonstrate, for the first time, that P_{25}/AuNPs framework on electrodes can offer a highly sensitive impedimetric platform for the detection of ZAP70 gene levels to diagnose and distinguish type of CLL patients by a genoassay. The designed aptasensor involves a simple and robust electrode modification and offers high

sensitivity and reproducibility. The developed DNA biosensor was able to differentiate between Ig-mutated and Ig-unmutated CLL and it was label-free, requiring no labeling process or external indicators. Thus, the presented impedimetric genosensor has the potential to be clinically useful for diagnosis of type of CLL in serum samples. Although the sensors for diagnosos and detection of CLL have been reported by some researchers (Labib et al., 2015, 2013; Ensafi et al., 2011; Lin et al., 2007), as the date of this manuscript, this is the first sensor that effectively differentiates to Ig-mutated and Ig-unmutated CLL. The developed DNA biosensor offers a more convenient research tool for the identification of two types of CLL. Our future research will focus on to design high-throughput clinical testing devices based on microarray and lab on chip technology and also produce suitable kits.

Acknowledgments

The authors wish to thank the Research Council of Isfahan University of Technology (IUT), the Center of Excellence in Sensor and Green Chemistry, and the Iranian Nanotechnology Initiative Council for their support.

References

Akhavan, O., Ghaderi, E., Rahighi, R., 2012. ACS Nano 6, 2904–2916.
Alfonta, L., Katz, E., Willner, I., 2000. Anal. Chem. 72, 927–935.
Ali, M.E., Mustafa, S., Che Man, Y.B., Adam, K.N., Humayun, K.N., 2014. J. Exp. Nanoscl. 9, 152–160.
Bia, S., Zhang, Z., Dong, Y., Wang, Z., 2015. Biosens. Bioelectron. 65, 139–144.
Campregher, P.V., Hamerschlak, N., 2014. Clin. Lymphoma Myeloma Leuk. 14, 271–276.
Chun, L., Kim, S.E., Cho, M., Cheo, W.S., Nam, J., Lee, D.W., Lee, Y., 2013. Sens. Actuators B 186, 446–450.
Crespo, M., Bosch, F., Villamor, N., Bellosillo, B., Colomer, D., Rozman, M., Marcé, S., López-Guillermo, A., Campo, E., Montserrat, E., 2003. N. Engl. J. Med. 348, 1764–1775.
Ensafi, A.A., Amini, M., Rezaei, B., 2014. Biosens. Bioelectron. 53, 43–50.
Ensafi, A.A., Heydari-Bafrooei, E., Rezaei, B., 2013. Anal. Chem. 85, 991–997.
Ensafi, A.A., Taei, M., Rahmani, H.R., Khayamian, T., 2011. Electrochim. Acta 56, 8176–8183.
Esencay, M., Hamad, B., 2015. Nat. Rev. Drug Discov. 14, 381–382.
Keller, G.H., Manak eds, M.M., 1993. DNA Probes. Stock-ton Press, New York.
Labib, M., Ghobadloo, S.M., Khan, N., Kolpashchikov, D.M., Berezovski, M.V., 2013. Anal. Chem. 85, 9422–9427.
Labib, M., Khan, N., Berezovski, M.V., 2015. Anal. Chem. 87, 1395–1403.
Lee, L.G., Connell, C.R., Bloch, W., 1993. Nucleic Acids Res. 21, 3761–3766.
Li, C.M., Chen, W., Yang, X., Sun, C.Q., Gao, C., Zheng, Z.X., Sawyer, J., 2005. Front. Biosci. 10, 2518–2526.
Lin, X.H., Wu, P., Chen, W., Zhang, Y.F., Xia, X.H., 2007. Talanta 72, 468–471.
Matthews, C., Catherwood, M., Morris, T.C., Alexander, H.D., 2004. Leuk. Lymphoma 2004 (45), 1899–1904.
Miller, S.A., Dykes, D.D., Polesky, H.F., 1998. Nueleic Acids Res. 16, 1215–1230.
Montserrat, E., 2006. Hematol. Am. Soc. Hematol. Educ. Program, 279–284.
Moreno, C., Montserrat, E., 2008. Blood Rev. 22, 211–219.
Moreno, C., Montserrat, E., 2010. Haematologica 95, 12–15.
Ozsoz, M., Erdem, A., Kerman, K., Ozkan, D., Tugrul, B., Topcuoglu, N., Ekren, H., Taylan, M., 2003. Anal. Chem. 75, 2181–2187.
Put, N., Konings, P., Rack, K., Jamar, M., Van Roy, N., Libouton, J.M., Vannuffel, P., Sartenaer, D., Ameye, G., Speleman, F., Herens, C., Poirel, H.A., Moreau, Y., Hagemeijer, A., Vandenberghe, P., Michaux, L., 2009. Genes Chromosom. Cancer 48, 843–853.
Rassenti, L.Z., Huynh, L., Toy, T.L., Chen, L., Keating, M.J., Gribben, J.G., Neuberg, D.S., Flinn, I.W., Rai, K.R., Byrd, J.C., Kay, N.E., Greaves, A., Weiss, A., Kipps, T.J., 2004. N. Engl. J. Med. 351, 893–901.
Rosenwald, A., Alizadeh, A.A., Widhopf, G., Simon, R., Davis, R.E., Yu, X., Yang, L., Pickeral, O.K., Rassenti, L.Z., Powell, J., Botstein, D., Byrd, J.C., Grever, M.R., Cheson, B.D., Chiorazzi, N., Wilson, W.H., Kipps, T.J., Brown, P.O., Staudt, L., M., 2001. J. Exp. Med. 194, 1639–1647.
Sadik, O.A., Aluoch, A.O., Zhou, A., 2009. Biosens. Bioelectron. 24, 2749–2765.
Scupoli, M.T., Pizzolo, G., 2015. Expert Rev. Hematol. 3, 341–348.
Slack, G.W., Wizniak, J., Dabbagh, L., Shi, X., Gelebart, P., Lai, R., 2007. Arch. Pathol. Lab. Med. 131, 50–56.
Šoljić, V., Beljan, P.R., Vukojević, K., Saraga-Babić, M., Bubalo, P., Karan, D., Todorović, J., Batinić, D., 2013. Leuk. Lymphoma 54, 1171–1176.
Strefford, J.C., 2015. Br. J. Haematol. 169, 14–31.
Tobin, G., Rosenquist, R., 2005. Med. Oncol. 22, 217–228.
Vroblova, V., Smolej, L., Krejsek, J., 2012. Hematology 17, 268–274.
Wang, Y., Fan, L., Xu, W., Li, J., 2012. Clin. Exp. Med 12, 69–77.
Zhang, K., Zhang, L., 2008. Electroanalysis 20, 2127–2133.
Zhang, Z., Xu, K., Xin, Y., Zhang, Z., 2015. Anal. Biochem. 476, 26–28.
Zhu, X., Li, J., He, H., Huang, M., Zhang, X., Wang, S., 2015. Biosens. Bioelectron. . http://dx.doi.org/10.1016/j.bios.2015.04.069